Chapter 15

Modulation of Multivalent Protein Binding on Surfaces by Glycopolymer Brush Chemistry

Kai Yu, A. Louise Creagh, Charles A. Haynes, and Jayachandran N. Kizhakkedathu

Abstract

The presentation of carbohydrates on an array can provide a means to model (mimic) oligosaccharides found on cell surfaces. Tuning the structural features of such carbohydrate arrays can therefore be used to help to elucidate the molecular mechanisms of protein-carbohydrate recognition on cell surfaces. Here we present a strategy to directly correlate the molecular and structural features of ligands presented on a surface with the kinetics and affinity of carbohydrate–lectin binding. The Surface Plasmon Resonance (SPR) spectroscopy analysis identified that by varying the spatial distribution (3D organization) of carbohydrate ligands within the surface grafted polymer layer, the mode of binding changed from multivalent to monovalent: a near 1000-fold change in the equilibrium association constant was achieved. The rupture forces measured by atomic force microscopy (AFM) force spectroscopy also indicated that the mode of binding between lectin and carbohydrate ligands can be modulated by the organization of carbohydrate ligands within the glycopolymer brushes.

Key words Glycopolymers, Polymer brush, Lectin, Carbohydrate, Binding kinetics

1 Introduction

The interaction of lectins and other carbohydrate-binding proteins with glycoproteins, glycolipids or polysaccharides displayed on a cell surface mediate a variety of biological processes such as cell signaling, cell adhesion, fertilization, and inflammatory responses [1–3]. Since the affinity of single carbohydrate residue and a protein is usually weak, multivalent interactions are often used by the nature by displaying multiple ligands or by the use of multivalent proteins [4–8]. Multivalency is often achieved through chelating effect [6–8] and proximity/statistical effect [9]. The increase in the affinity is thought to be dependent on the structure of the lectin [10], the density of the carbohydrate ligands and the manner in which they are presented on the cell surface [11–13]. An improved understanding of the contribution of the molecular

and structural features of ligands presented on a surface to the mechanisms of carbohydrate–protein recognition would therefore be of great use, in part by helping to resolve their roles in various biological processes.

While improvements in the affinity of multivalent lectins for carbohydrates presenting surfaces have been achieved, our fundamental understanding of the reaction mechanism connecting binding affinity/avidity and surface structure remains poor. This limitation could be addressed through the development of carbohydrate arrays where the binding interactions can be tuned from monovalent to multivalent using chemistry that allows for precise control of the presentation of the ligands on a surface. The implementation of such a technology would permit direct correlation of binding affinity/avidity with engineered changes in the surface structure, and thereby aid the design and development of potent lectin inhibitors and biological effectors.

In this study, we therefore report on a strategy to modulate multivalent interactions at the surfaces by changing the spatial arrangement of carbohydrate residues (mannose and galactose) within end-grafted glycopolymer brushes [14]. Glycopolymer brushes with pendent sugar residues (Fig. 1) are synthesized with tight control of grafting density, degree of polymerization, and carbohydrate composition; all these parameters are independently controlled. These systems offer an opportunity to mimic the cell surface glycocalyx, as sugar units along each grafted polymer chain is presented in a manner similar to proteoglycans presented on the cell surface. A systematic investigation on the interaction of *Concanavalin A* (*Con A*), a bivalent lectin, with glycopolymer brushes was conducted using SPR to explore the influence of molecular and structural features of the surface on binding characteristics. Binding equilibrium and kinetic data collected by SPR are reported and are used to determine equilibrium, forward and reverse rate constants for each possible association/dissociation
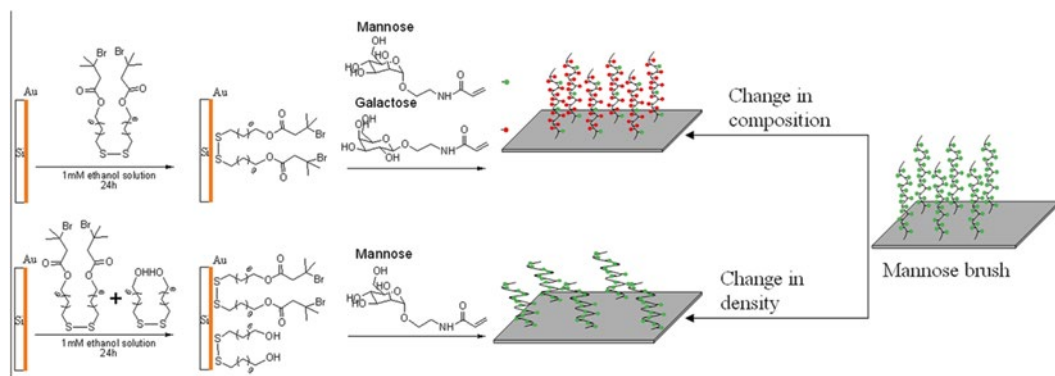

Fig. 1 Synthesis of glycopolymer brush with different composition and grafting density

reaction that can occur between bivalent Con A and the grafted brush layer displaying the binding partner, mannose. The intermolecular unbinding force between Con A and carbohydrate units on the surface is also investigated by AFM force spectroscopy.

2 Materials

2.1 Chemicals

1. 2′-acrylamidoethyl-α-D-mannopyranoside (AAEM, mannose monomer) and 2′-acrylamidoethyl-β-D-galactopyranoside (AAEGal, galactose monomer) are synthesized by a procedure as reported previously [15].

2. Copper (I) chloride (99 %, Sigma-Aldrich) is purified by washing with acetic acid, methanol and dried under vacuum.

3. Copper (II) chloride (99 %, Sigma-Aldrich).

4. Tris (2-(dimethylamino)ethyl)amine (Me$_6$TREN) (97 %, Sigma-Aldrich).

5. Methyl 2-chloropropionate (97 %, Sigma-Aldrich).

6. 2-bromo-2-isobutyryl bromide (98 %, Sigma-Aldrich).

7. Manganese (II) chloride (99 %, Sigma-Aldrich).

8. Calcium chloride (99 %, Sigma-Aldrich).

9. D-(+)-mannose (99 %, Sigma-Aldrich).

10. Phosphoric acid solution (85 wt% in H$_2$O, Sigma-Aldrich).

11. Triethylamine (Et$_3$N) (99 %, Sigma-Aldrich).

12. Ethanolamine hydrochloride (99 %, Sigma-Aldrich).

13. DMSO (99 %, Sigma-Aldrich).

14. NHS-PEG6000-NHS (Rapp Polymere GmbH, Germany).

15. Surface ATRP initiator (BrC-(CH$_3$)$_2$COO(CH$_2$)$_{11}$S)$_2$ (SAM-Br) and (HO(CH$_2$)$_{11}$S)$_2$ (SAM-OH) are synthesized by using a similar procedure reported in the literature [16].

2.2 Other Commercial Regents

1. SPR chip: Bare gold chip (BIAcore SIA kit Au, Catalog No. BR-1004-05) is purchased from GE Healthcare.

2. SPR Maintenance kit (BR-1006-66) is purchased from GE Healthcare.

3. AFM probes with spring constant about 0.06 N/m are purchased from Veeco, US.

2.3 Buffering Solutions

1. 150 mM phosphate buffered solution, pH 4.8, 137 mM NaCl, 10 mM phosphate, 2.7 mM KCl, containing 1 mM CaCl$_2$ and 1 mM MnCl$_2$.

2. 25 mM phosphate buffered solution, pH 4.8.

3. 25 mM phosphate buffered solution, pH 7.4.

4. 5 M mannose buffer solution.

5. 100 mM phosphoric acid solution.

2.4 Proteins	Concanavalin A from *Canavalia ensiformis* (Jack bean) Type IV, lyophilized powder (Sigma).

3   Methods

3.1 Preparation of Glycopolymer Brushes on Au Chips	The glycopolymer brushes with different composition and grafting density were grown on initiator modified SPR bare Au chip by surface-initiated atom transfer radical polymerization through changing the monomer composition and initiator density. End-grafted galactose-based copolymers were prepared with increasing amounts of mannose to investigate the influence of various characteristics of the glyco-structures on carbohydrate binding of the lectin, Con A. Galactose is a neutral sugar which has no specific binding interaction with Con A and was therefore be used to dilute the ligand concentration within the brush without affecting the properties of brush structure such as hydration and steric factors. In addition, mannose homopolymer brushes with different grafting density were prepared to investigate whether steric factors influence the binding characteristics.

SPR Analyses: SPR measurements were performed on a BIAcore 3000 (BIAcore, Uppsala, Sweden) operated using the BIAcore control software. The flow rate of analyte solution and 150 mM PBS buffer (pH 4.8, containing 1 mM Ca^{2+}, 1 mM Mn^{2+}) through the flow cells was set at 30 μL/min. A series of 750 μL Con A solutions were injected and allowed to flow through the channels. The concentration of each injection varied from 0.05 to 150 μM. There was no regeneration between consecutive injections (Fig. 2a). The pAAEGal brush modified gold chip was set as the reference surface since there was no specific interaction observed between Con A and pAAEGal brushes. The response difference between mannose and galactose polymer brush modified surfaces was taken as the response due to the specific interaction between Con A and mannose containing brush. The equilibrium response was determined from duplicate measurements and plotted against the analyte concentration, and fitted to a model with Hill slope ([17], Eq. 1) by using the GraphPad Prism 5 to determine the association constant (Table 1) [14].

$$\mathrm{RU} = \mathrm{RU_{max}} \frac{C^b}{K_D + C^b} \tag{1}$$

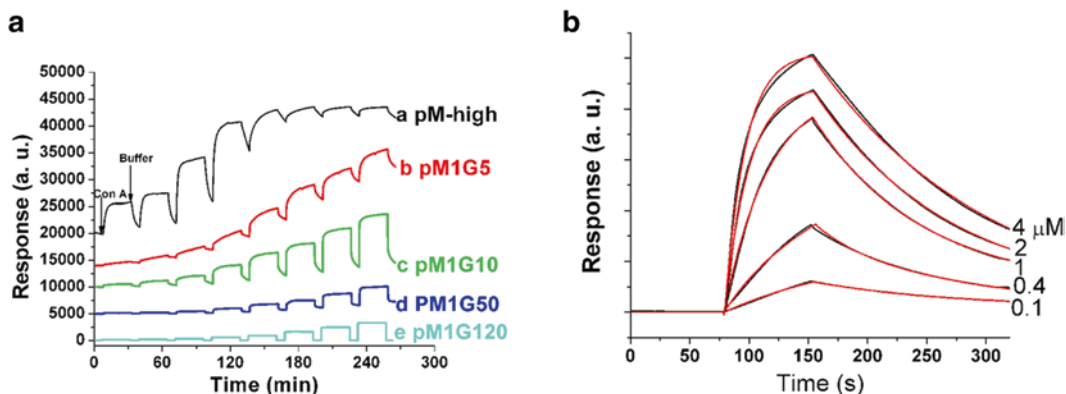**Fig. 2** (**a**) SPR sensorgram for the interaction of Con A with glycopolymer layers with different mannose contents: (a) 100 %; (b) 16.7 %; (c) 9 %; (d) 2 %; and (e) 0.8 %. For the copolymer layers composing of 100 and 16.7 % mannose, eight different concentrations (in the sequence of injection, 0.1, 0.2, 0.4, 1, 4, 10, 20, 50 μM) of Con A was injected and flowed through. For the copolymer layers composing of 9 % and 2 % mannose, eight different concentrations (1, 2, 4, 10, 20, 32, 64, 108 μM) of Con A was injected and flowed through the channel. For the copolymer layer composing of 0.8 % mannose, eight different concentration (1, 4, 10, 20, 32, 64, 108, 150 μM) of Con A was injected and flowed through the channel. (**b**) Kinetics analyses of Con A binding to glycopolymer layers. Shown are experimental data (*black curves*) and the derivation of the fitted sensorgram (*red lines*) by bivalent model fitting of Con A binding to glycopolymer layers with mannose content 100 %. Reproduced with permission from Yu K, Creagh AL, Haynes CA, Kizhakkedathu JN (2013) *Anal Chem* 85, 7786–7793. Copyright (2013) American Chemistry Society

where K_D ($=1/K_A$) is the equilibrium dissociation constant, h is the Hill coefficient, RU is the steady-state SPR response to a solution of Con A of concentration C, and RU_{max} is the maximal SPR response brought by binding extrapolated to the saturation concentration of lectin.

For the calculation of the association rate constant and dissociation rate constant, a conventional regeneration protocol was used. After each injection of Con A solution, the chip was regenerated (Fig. 2b). The association and dissociation rate constants were derived by fitting the data to a bivalent analyte model using the BIAevaluation Software, version 4.1. Bulk refractive index effect brought by variation of analyte concentration was fixed during the fitting. The bulk effect was measured by allowing analyte solution flow through the reference sample-galactose brush modified chip. The dissociation rate constant for the interaction between Con A and brush presenting 0.8 % mannose was obtained by fitting the data to one phase exponential decay with using Origin 7.0 software [14].

3.2 AFM Force Spectroscopy Studies of Lectin Binding to Glycopolymer Brushes

Glycopolymer brushes having compositions and structures similar to those employed in the SPR analyses were utilized. AFM tips were functionalized with Con A using PEG as a spacer. The approach and retraction force curves for a Con A-coupled AFM tip to either an all mannose brush or an all galactose brush were

Table 1

Equilibrium association constant (K_A) and Hill coefficient (h) data for binding of Con A to various end-grafted glycopolymers

Samples	Mannose composition (%)	Grafting density, σ, (chains/nm²)	Association constant (K_A) from Eq. 1 (M⁻¹)	Association constant (K_A) from kinetic study (M⁻¹)	h
pM-low	100	0.006	$(7.4 \pm 1.3) \times 10^5$	N/D	0.55 ± 0.14
pM-med	100	0.02	$(1.5 \pm 0.6) \times 10^6$	N/D	0.71 ± 0.09
pM-high	100	0.10	$(3.1 \pm 0.5) \times 10^6$	5.5×10^6	0.69 ± 0.12
pM1G5	16.7	0.09	$(1.2 \pm 0.5) \times 10^5$	6.2×10^5	0.65 ± 0.06
pM1G10	9	0.08	$(3.1 \pm 0.2) \times 10^4$	N/D	0.80 ± 0.05
pM1G20	4.8	0.09	$(2.6 \pm 0.3) \times 10^4$	5.2×10^4	0.83 ± 0.04
pM1G50	2	0.09	$(8.4 \pm 0.3) \times 10^3$	9.2×10^3	0.96 ± 0.06
pM1G120	0.8	0.09	$(3.8 \pm 0.6) \times 10^3$	4.2×10^3	0.99 ± 0.10

Reprinted with permission from Yu K, Creagh AL, Haynes CA, Kizhakkedathu JN (2013) *Anal Chem* 85, 7786–7793. Copyright (2013) American Chemistry Society
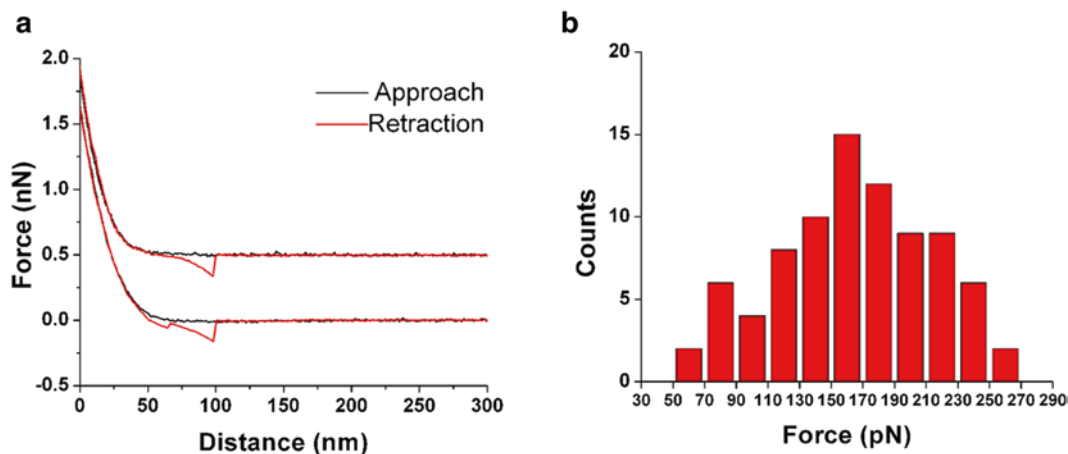

Fig. 3 (**a**) Representative approach (*black line*) and retraction (*red line*) force curves for the interaction of mannose polymer layer ($\sigma = 0.1$ chains/nm² and height = 59 nm) with Con A modified tip. (**b**) Probability distribution histograms of the maximum unbinding force during retracting Con A modified tip from mannose polymer layer. Reprinted with permission from Yu K, Creagh AL, Haynes CA, Kizhakkedathu JN (2013) *Anal Chem* 85, 7786–7793. Copyright (2013) American Chemistry Society

recorded (Fig. 3). On tip approach, the onset of the region of constant compliance was used to determine the zero distance, and on retraction the region in which the force was unchanged was used to determine the zero force. The rate of tip-sample approach or retraction was set as 0.5 μm/s. The raw AFM force data (cantilever

deflection vs. displacement data) were converted into force vs. separation following the principle of Ducker et al. by using custom Matlab v.5.3 (Math Works, Natick, MA) software [18]. The software converts the cantilever deflection vs. linear voltage displacement transformer signal into restoring force vs. tip-substrate separation using user input trigger and spring constant values. We followed our published protocol for the calculations of the adhesive force [19].

3.3 Preparation of End-Grafted Glycopolymer on SPR Chip

3.3.1 Preparation of Initiator Modified Gold Chip

1. Clean Gold coated chips first by soaking in chromic acid for 1 h. Then wash the chips with water and dry under a stream of argon.

2. Deposit self-assembled monolayers onto the gold by immersing the cleaned gold chips in 1 mM SAM-Br or mixtures of SAM-Br and SAM-OH overnight at room temperature (22 °C).

3. Wash the initiator modified chips thoroughly with ethanol and THF and dry in an argon flow.

3.3.2 Synthesis of pAAEM Layers on the Initiator Modified Au Chip

1. Add copper (II) chloride ($CuCl_2$, 1.35 mg, 0.01 mmol), copper (I) chloride (CuCl, 8 mg, 0.08 mmol), Me_6TREN (52 μL, 0.18 mmol) successively into a glass tube followed by Milli-Q water (12 mL).

2. Degas the catalyst solution with three freeze–pump–thaw cycles.

3. Transfer the solution into a glove box.

4. Draw aliquots of the catalyst solution (1.5 mL) and add into the vials which contained 2′-acrylamidoethyl-α-D-mannopyranoside (75 mg). After the monomer was completely dissolved, immerse the ATRP initiator modified gold chip fully into the solution.

5. Add 20 μL of a solution of methyl 2-chloropropionate in methanol (250 μL in 5 mL methanol) to the reaction solution.

6. Allow the surface-initiated polymerization to proceed at RT (22 °C) for 24 h.

7. Rinse the substrates with water thoroughly, followed by drying under a flow of argon gas.

8. The solution was dialyzed against deionized water, and then freeze-dry. *See* **Note 1** for overall.

3.4 SPR Measurements

3.4.1 SPR Equilibrium Studies

1. Assemble the brush modified chip onto the chip holder and dock into the SPR instrument.

2. Normalize signal response by using BIAnormalzing solution provided in the maintenance kit.

3. Inject buffer (150 mM phosphate buffered solution, pH 4.8, with 1 mM $CaCl_2$ and 1 mM $MnCl_2$) and allow to flow through

the channels of SPR chip until the baseline stabilized with changes less than 1RU/min.

4. Inject a series of 750 μL Con A solutions (0.05–150 μM) at a flow rate of 30 μL/min and allowed to flow through the channels without regeneration between consecutive injections.

5. Undock the chip and replace with maintenance chip.

6. Desorb procedure is done using the desorb solution 1 and 2 providing in the maintaining kit. *See* **Note 2** for overall.

3.4.2 SPR Kinetic Studies

The procedure is similar to the SPR equilibrium study except that Con A solution is injected and allowed to flow through the channels. After each injection, the chip is regenerated by 300 μL 5 M mannose buffer solution twice and 10 μL 0.1 M phosphoric acid. *See* **Note 3** for overall.

3.5 AFM Force Spectroscopy

3.5.1 AFM Tip Modification

1. Clean AFM tips by O_2 plasma at 50 W for 60 s.

2. Immerse the AFM tips overnight in a solution of ethanolamine hydrochloride in DMSO (5.5 g in 10 mL) to generate amino groups on the tip surface.

3. Rinse the tips in chloroform and incubate in a chloroform solution containing NHS-PEG6000-NHS (10 mg/mL) containing 0.5 % Et_3N.

4. Rinse the tips with chloroform, dry with argon and immerse in 25 mM phosphate buffer (pH 7.4) containing Con A (2 mg/mL). After 2 h, remove the tips from incubation and wash it briefly in 25 mM phosphate buffer (pH 7.4) and then with 25 mM phosphate buffer (pH 4.8).

3.5.2 AFM Force Measurements

1. Mount the brush modified substrate on the stage using an AFM steel punk and sticky tab.

2. Attach the Con A modified tip to the cantilever holder on a wet cell.

3. Injected buffer solution (150 mM phosphate buffered solution, pH 4.8, with 1 mM $CaCl_2$ and 1 mM $MnCl_2$) through the hole of the wet cell to make the cantilever and samples fully wetted.

4. After laser alignment and photodiode alignment, set scanning parameters and engaging the microscope and bring the tips in contact with the substrate for 10 min.

5. Collect force curves with ramp size of 500 nm and rate of tip-sample approach or retraction was set as 0.5 μm/s. *See* **Note 4** for overall.

4   Notes

1. Poly(2′-acrylamidoethyl-β-D-galactopyranoside) (pAAEGal) layers and copolymers of 2′-acrylamidoethyl-α-D-mannopyranoside and 2′-acrylamidoethyl-β-D-galactopyranoside P(AAEM-*co*-AAEGal) layers with different molar feed ratios of AAEM to AAEGal (1:5, 1;10, 1:20, 1:50, and 1: 120) are synthesized using a similar procedure. All the layer structures are characterized in terms of thickness, grafting density, and molecular weight (Table 2).

Table 2
Characteristics of pAAEM (pM, M-mannose) layers and p(AAEM-*co*-AAEGal) (pM$_X$G$_Y$, M-mannose, G-galactose) layers

Samples	Feed ratio of AAEM (mannose) to AAEGal (galactose)	Mannose composition (%)	Dry thickness (nm)	Grafting density, σ^a (chains/ nm^2)	Molecular weight of free polymer (Mn) (Mw/Mn)	Distance between the chains, d^b (nm)	Equilibrium thickness, Le^c (nm)
pM-high	100, 0	100	19.6	0.10	123 000 (1.3)	3.2	59 ± 3.6
pM-med	100, 0	100	4.6	0.02	130 000 (1.3)	7.1	15.5 ± 0.7
pM-low	100, 0	100	1.3	0.006	130 000 (1.3)	12.9	N/D
pM1G5	1, 5	16.7	20	0.09	131 000 (1.3)	3.3	74 ± 5.7
pM1G10	1, 10	9	16.3	0.08	122 000(1.4)	3.5	55 ± 3.2
pM1G20	1, 20	4.8	22	0.09	141 000 (1.4)	3.3	67 ± 4.7
pM1G50	1, 50	2	23	0.09	148 000 (1.3)	3.3	71 ± 6.3
pM1G120	1, 120	0.8	17	0.09	118 000 (1.4)	3.3	58 ± 5.1
pG	0, 100	0	24.4	0.09	158 000 (1.3)	3.3	70 ± 2.7

^{a}The grafting density (σ) for glycopolymer layers was estimated by using the equation, $\sigma = (h\rho N_A)/Mn$, where Mn is the molecular weight of free polymer in the solution, N_A is the Avogado's number, h is the polymer layer thickness measured by ellipsometer, ρ is the density of glycopolymer (we assumed the density of glycopolymer is equal to 1 g/cm^3)

^{b} $$d = \frac{1}{\sqrt{\sigma}} \text{nm}$$

^{c}Equilibrium thickness (Le) was determined by AFM as the critical distance from the substrate surface beyond which no repulsive force was detectable. *N/D* not determined. Reprinted with permission from Yu K, Creagh AL, Haynes CA, Kizhakkedathu JN (2013) *Anal Chem* 85, 7786–7793. Copyright (2013) American Chemistry Society

2. Procedure for the calculation of binding constant was described in the method section SPR analyses.

3. The bulk effect was measured by allowing analyte solution flow through the reference sample-galactose layer modified chip. Procedure for calculation of the association and dissociation rate constants was described in the previous method section on SPR analyses.

4. The conversion of raw AFM force data to force vs. separation and the calculations of the adhesive force are given in the section "AFM force spectroscopy studies of lectin binding to glycopolymer brushes." The spring constant for the AFM cantilever was measured using thermal equipartition theorem [20]. The force curves collected on the galactose brush was used to observe the no specific interaction.

Acknowledgments

References

1. Sharon N, Lis H (2004) History of lectins, from hemagglutinins to biological recognition molecules. Glycobiology 14:53R–62R

2. Bertozzi CR, Kiessling LL (2001) Chemical glycobiology. Science 291:2357–2364

3. Dube DH, Bertozzi CR (2005) Glycans in cancer and inflammation – potential for therapeutics and diagnostics. Nat Rev Drug Discov 4:477–488

4. Mandal DK, Kishore N, Brewer CF (1994) Thermodynamics of lectin-carbohydrate interactions. titration microcalorimetry measurements of the binding of N-linked carbohydrates and ovalbumin to concanavalin A. Biochemistry 33:1149–1156

5. Schwarz FP, Puri KD, Bhat RG, Surolia A (1993) Thermodynamics of monosaccharide binding to concanavalin A, pea (Pisum sativum) lectin, and lentil (Lens culinaris) lectin. J Biol Chem 268:7668–7677

6. Mammen M, Choi SK, Whitesides GM (1998) Polyvalent interactions in biological systems, implications for design and use of multivalent ligands and inhibitors. Angew Chem Int Ed 37:2755–2794

7. Lundquist JJ, Toone EJ (2002) The cluster glycoside effect. Chem Rev 102:555–578

8. Dam TK, Brewer CF (2008) Effects of clustered epitopes in multivalent ligand-receptor interactions. Biochemistry 47:8470–8476

9. Wolfenden ML, Cloninger MJ (2006) Carbohydrate-functionalized dendrimers to investigate the predictable tunability of multivalent interactions. Bioconjugate Chem 17:958–966

10. Ting SRS, Chen G, Stenzel MH (2010) Synthesis of glycopolymers and their multivalent recognitions with lectins. Polym Chem 1:1392–1412

11. Godula K, Bertozzi CR (2012) Density variant glycan microarray for evaluating cross-linking

of mucin-like glycoconjugates by lectins. J Am Chem Soc 124:15732–15742

12. Wilczewski M, Van der Heyden A, Renaudet O, Dumy P, Coche-Guerente L, Labbe P (2008) Promotion of sugar–lectin recognition through the multiple sugar presentation offered by regioselectively addressable functionalized templates (RAFT), a QCM-D and SPR study. Org Biomol Chem 6:1114–1122

13. Wang X, Ramstrom O, Yan MD (2010) Quantitative analysis of multivalent ligand presentation on gold glyconanoparticles and the impact on lectin binding. Anal Chem 82:9082–9089

14. Yu K, Creagh AL, Haynes CA, Kizhakkedathu JN (2013) Lectin interactions on surface-grafted glycostructures, influence of the spatial distribution of carbohydrates on the binding kinetics and rupture forces. Anal Chem 85:7786–7793

15. Yu K, Kizhakkedathu JN (2010) Synthesis of functional polymer brushes containing carbohydrate residues in the pyranose form and their specific and nonspecific interactions with proteins. Biomacromolecules 11:3073–3085

16. Shah RR, Merreceyes D, Husemann M, Rees I, Abbott NL, Hawker CJ, Hedrick JL (2000) Using atom transfer radical polymerization to amplify monolayers of initiators patterned by microcontact printing into polymer brushes for pattern transfer. Macromolecules 33: 597–605

17. Dam TK, Gerken TA, Brewer CF (2009) Thermodynamics of multivalent carbohydrate-lectin cross-linking interactions, importance of entropy in the bind and jump mechanism. Biochemistry 48:3822–3827

18. Ducker WA, Sendan TJ, Pashley RM (1992) Measurement of forces in liquids using a force microscope. Langmuir 8:1831–1835

19. Zou YQ, Rossi NAA, Kizhakkedathu JN, Brooks DE (2009) Barrier capacity of hydrophilic polymer brushes to prevent hydrophobic interactions, effect of graft density and hydrophilicity. Macromolecules 42:4817–4828

20. Wang M, Cao Y, Li HB (2006) The unfolding and folding dynamics of TNfnALL probed by single molecule force-ramp spectroscopy. Polymer 47:2548–2554